Naval Research Laboratory

Washington, DC 20375-5000

NRL Report 9326

Radar Pulse Compression and Electromagnetic Interference (EMI)

CHING-TAI LIN

Search Radar Branch
Radar Division

May 30, 1991

Approved for public release; distribution unlimited.

REPORT DOCUMENTATION PAGE

Form Approved
OMB No. 0704-0188

1. AGENCY USE ONLY *(Leave blank)*	2. REPORT DATE	3. REPORT TYPE AND DATES COVERED
	May 30, 1991	Interim

4. TITLE AND SUBTITLE

Radar Pulse Compression and Electromagnetic Interference (EMI)

5. FUNDING NUMBERS

PE - 605803N
PR - S0706

6. AUTHOR(S)

Ching-Tai Lin

7. PERFORMING ORGANIZATION NAME(S) AND ADDRESS(ES)

Naval Research Laboratory
Washington, DC 20375-5000

8. PERFORMING ORGANIZATION REPORT NUMBER

NRL Report 9326

9. SPONSORING/MONITORING AGENCY NAME(S) AND ADDRESS(ES)

Space and Naval Warfare Systems Command
Washington, DC 20365-5100

10. SPONSORING/MONITORING AGENCY REPORT NUMBER

11. SUPPLEMENTARY NOTES

12a. DISTRIBUTION/AVAILABILITY STATEMENT

12b. DISTRIBUTION CODE

13. ABSTRACT *(Maximum 200 words)*

A practical example of using a transmission filter to eliminate electromagnetic interference (EMI) is analyzed for a possible upgraded SPS-49 system. In addition, in contrast to conventional methodology, a fundamental approach to eliminating EMI based on signal formating is presented. It is shown that use of complementary coded signals with appropriate waveform synthesis may significantly reduce radar EMI without degrading the radar's primary function of detecting targets.

14. SUBJECT TERMS

Electromagnetic interference
EMI
Radar pulse compression
Complementary code

15. NUMBER OF PAGES

27

16. PRICE CODE

17. SECURITY CLASSIFICATION OF REPORT	18. SECURITY CLASSIFICATION OF THIS PAGE	19. SECURITY CLASSIFICATION OF ABSTRACT	20. LIMITATION OF ABSTRACT
UNCLASSIFIED	UNCLASSIFIED	UNCLASSIFIED	SAR

NSN 7540-01-280-5500

Standard Form 298 (Rev 2-89)
Prescribed by ANSI Std 239-18
298-102

CONTENTS

1. INTRODUCTION 1

2. TRADEOFFS BETWEEN RADAR PERFORMANCE AND EMI SUPPRESSION 2

3. A FUNDAMENTAL APPROACH TO ELIMINATING EMI 11

   3.1 A Class of Complementary Codes 11
   3.2 Advanced Waveform Synthesis 15

4. DISCUSSION AND CONCLUSION 22

5. ACKNOWLEDGMENTS 22

6. REFERENCES 22

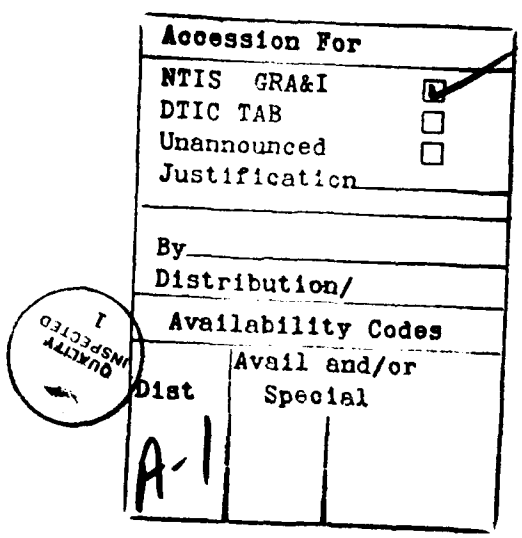

RADAR PULSE COMPRESSION AND ELECTROMAGNETIC INTERFERENCE (EMI)

1. INTRODUCTION

Electromagnetic interference (EMI) is a well-known problem that affects most radar and telecommunication systems. In the past, radars have had relatively narrow bandwidths and EMI between radars was kept to a minimum by frequency allocation to different frequency bands. However, the current trend is toward wide operating agile and instantaneous bandwidths, possibly 50% or more, which necessarily overlap. EMI reduction therefore requires other means than frequency allocation to different bands, possibly noninterfering coded waveforms, as pursued in this report.

EMI, in a broad sense, includes intrasystem problems as well as intersystem problems. A number of solutions have been used or proposed to reduce EMI, based on the characteristics of radiated interference, transmission path, and receiver configuration. They also depend on how the problems are defined, that is, from the viewpoint of signal transmission, signal reception, or both. The general methodology may include: (1) grounding and bonding, (2) shielding, (3) use of radiation absorption material (RAM) or chemical agent, (4) filtering, (5) frequency management, (6) interference cancellation system (ICS), (7) equipment design such as the use of multicouplers, (8) advanced signal processing via state-of-the-art technology and expert systems, and many others. From a radar aspect, the electromagnetic interference is considered to be externally generated and does not include clutter and intrasystem noise. Generally, differences between desired signals and multipath/externally generated signals can be used to suppress the interference and to augment the desired signals. Typical interference suppressers are sidelobe blankers, defruiters, adaptive arrays, mainlobe notchers, transmission/predetection filters, coherent sidelobe cancellers or adaptive interference cancellers [1], which directly couple a sample of the interference waveform from the transmitter sources to the receiver.

To date, besides the above methodology, not much work has been reported in eliminating EMI from the viewpoint of basic signal structure. In this report, we propose a fundamental approach to eliminating EMI by applying complementary coded signals. We consider transmitted multiple-pulsed (dissimilar) waveforms as a burst of pulses that are pulse-compressed by complementary sequences. We then search a class of these characterized signals in which the property of *mutual orthogonality* is attained. As a result, different signals in a specifically derived set can be assigned to different radars on the same or different platforms in which the signals are mutually orthogonal *in the sense that cross-correlation of signals is zero.* Therefore, the interference from other radar sources may be reduced. Since the derived/applied signals are all complementary coded waveforms, the individual signal, as we refer to its composed multiple pulses, is presented in an orthogonal matrix form. This implies that the signal autocorrelation (without considering Doppler shift) is zero at least over the unambiguous range except at the matched point. Thus, zero sidelobes of the stationary targets are attained. Specific waveforms in this category have the above property extended beyond the maximum unambiguous range. When the signal is continuously transmitted and matched to the reference for

Manuscript approved March 19, 1991.

specific range intervals, then the stationary clutter or targets from the mismatched range intervals are eliminated. The methodology described here provides a means of fundamentally eliminating EMI without degrading the radar performance.

In Section 2, effects caused by the use of pulse compression waveforms against electromagnetic interference are described. We consider a practical example of using a transmission filter for eliminating interference to the Air Traffic Control Radar Beacon System (ATCRBS) airborne Mode S transponder and Traffic Alert and Collision Avoidance System (TCAS) receiver in an upgraded SPS-49 system. Then, in Section 3, we detail the fundamental approach to eliminating EMI through the use of complementary coded signals. Advanced waveform synthesis is included in this section to solve imperfection of orthogonality in the presence of Doppler shift.

2. TRADEOFFS BETWEEN RADAR PERFORMANCE AND EMI SUPPRESSION

It is the current trend in radar design to have a relatively wide bandwidth (both operating agile bandwidth and instantaneous bandwidth). As a result, very high resolution can be achieved for radars to provide improved clutter suppression for the detection of small targets. Required peak power is reduced. In addition, unwanted EMI can be notched out through filtering or ICS. Pulse compression waveforms are thus widely used. The commonly used waveforms in radar are frequency, phase, or amplitude modulated. The popular pulse compression waveforms are:

(1) linear frequency modulation (chirp) waveforms,

(2) Barker and pseudorandom binary phase codes,

(3) step frequency modulation (step chirp) waveforms,

(4) step-frequency-derived polyphase codes such as Frank and P_1 codes,

(5) linear-frequency-derived polyphase codes such as P_3 and P_4 codes,

(6) complementary codes, and

(7) Huffman codes.

In the above, the complementary codes can be binary or polyphase codes and the Huffman codes are amplitude and phase modulated. For the unweighted linear chirp waveform, its autocorrelation function has the form of $\sin x / x$, which shows high peak sidelobes. However, the sidelobe level can be brought down by applying appropriate weighting functions, e.g., -42.8 dB peak sidelobe by using a Hamming weighting. The chirp waveforms have range-Doppler coupling properties and are Doppler tolerant.

The binary codes, however, have relatively poor sidelobes. For an aperiodic pseudorandom code of length N, the peak voltage sidelobe best obtainable is about $1/N$. It is the ideal case that the voltage sidelobe level reaches $1/N^2$ as seen in the Barker or periodic pseudorandom codes. However the binary phase-modulated waveforms are not Doppler tolerant. Other codes listed in (3) through (7) possess specific characteristics and may show combined favorable properties different from the forementioned codes. For example, the polyphase Frank codes have lower voltage sidelobes of about $1/(\pi^2 N)$ and are more Doppler tolerant than the binary codes. Many useful radar waveforms, with associated properties, are described in the literatures (e.g. [2-4]).

In Section 3, we discuss in detail the complementary codes, which when considered as multiple-pulsed (dissimilar) signals, appear to be promising for both suppressing EMI and detecting a target. In this section, the EMI solution is restricted to the conventional approach through the use of a transmission filter. Actually the use of a desired filter to eliminate interference will produce other effects detrimental to the radar performance. The portion of the signal that is filtered away is no longer part of the energy available for target detection. Also, a distortion of the pulse compression waveforms being used is unavoidable. These effects cause power loss and internal subcode interference. Here we examine how the radar performance, i.e., the matched filter output, is affected by the application of an EMI-suppressing filter and pulse compression waveforms.

In conjunction with the AN/SPS-49 waveforms and system architecture study [5], we assume that the operation bandwidth is 850 to 1400 MHz for a possible upgraded system. We also assume that a 360 kW transmitter is used. According to Ref. 6, the victim receivers considered for interference are the ATCRBS airborne Mode S transponder and the TCAS receiver. To eliminate EMI as seen from the aspect of signal transmission, a transmission filter (instead of a predetection filter) with the following characteristics must be applied. (See Table 1.)

Table 1 — Filter Rejection Characteristics

	Rejection Magnitude dB	Rejection Bandwidth MHz
ATCRBS Mode S Transponder (1030 MHz)	55	44
TCAS < Receiver (1090 MHz)	50	22

To examine how the matched filter output is affected by the this designed filter, we consider the applied waveform to be a step-frequency-derived polyphase Frank code with a code length of 100. This polyphase Frank code is the concatenation of unit pulses with their phases equal to

$$\phi_{ij} = \frac{2\pi}{N}(i - 1)(j - 1);\ j = 1, 2, \ldots 10 \text{ and } i = 1, 2, \ldots, 10 . \quad (1)$$

The reason to consider this waveform is that the Frank code, when applied as multiple-pulsed signals, is also a complementary code that appears to be promising in suppressing EMI (see Section 3). It is known that the receiver matched filter output, in the absence of noise and Doppler shift, is the response of signal autocorrelation; that is, the convolution of $\tilde{c}(t)$ with $c^*(t)$ as defined in Fig. 1(a), where $\tilde{c}(t)$ and $c^*(t)$ are the time reversal and complex conjugate of $c(t)$, respectively. The autocorrelation functions can also be obtained from the signal spectra through discrete Fourier transformation (DFT) as shown in Fig. 1(b).

The signal power spectrum of the 100-element Frank code is shown in Fig. 2(a). In the figure, the coded signal is oversampled five times and padded with 499 zeroes and then DFT processed according to Fig. 1(b). Therefore, there are 999 samples. The abscissa of the figure indicates the index over the frequency, and the frequency increment is the reciprocal of the sampling number (999) multiplied by the sampling spacing in time. The envelope of this waveform spectrum has the form of $(\sin x/x)^2$, and the first null appears at the frequency of $1/\tau$ where τ is the designed compressed-pulsewidth. The signal spectrum is further inverse-DFT processed to obtain the signal autocorrelation function, or the matched filter output, as shown in Fig. 2(b). In the figure and the corresponding ones through Fig. 7(b), the compressed pulse responses are obtained by sampling the wavform once-per-code-element (or per reciprocal bandwidth). The peak sidelobe is about −30 dB.

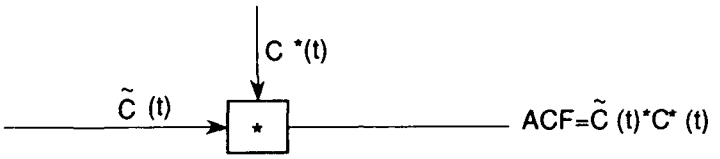

Fig. 1(a) — An autocorrelation function defined by signal convolution

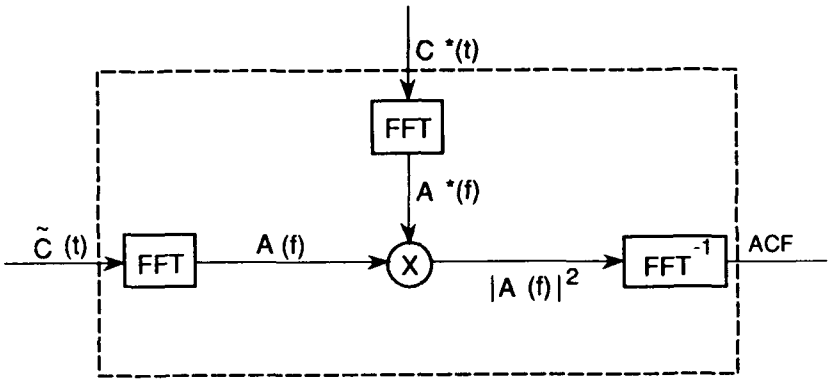

Fig. 1(b) — An autocorrelation function derived through DFT processing of signal spectra

As noted before, we assume that the signal spectrum of Fig. 2(a) has a bandwidth from 850 to 1400 MHz, approximately between the mainlobe nulls. Then the interference located at 1030 MHz and 1090 MHz (Table 1) can be easily visualized. We consider first that the interference is notched out by narrow bandstop filters of 1 MHz centered at 1030 MHz and 1090 MHz. Fig. 3(a) illustrates the resulting transmitted signal spectrum. Following Fig. 1(b) and performing DFT processes, we obtain a matched filter output as shown in Fig 3(b). The figure indicates nearly the same sidelobe level as in Fig. 2(b) and shows little performance degradation because of the use of a cancellation filter.

If the interference needs to be notched out by a filter of larger bandwidth such as specified in Table 1, then the corresponding transmitted signal and the resulting matched filter output are obtained in Fig. 4. It is shown that the peak sidelobe of the output response is raised to approximately -19 dB. Apparently the radar detection capability is substantially affected by the insertion of a filter for suppressing EMI. In a practical application, we may compensate somewhat by using a signal having a longer code length. Figures 5 through 7 (corresponding to Figs. 2 through 4) show the power spectra and the associated matched filter outputs for the Frank coded signal with a code length of 196 elements. The peak sidelobes are -32 and -24 dB, respectively, in the above narrow- and wide-passband notching cases (Fig. 6 and 7).

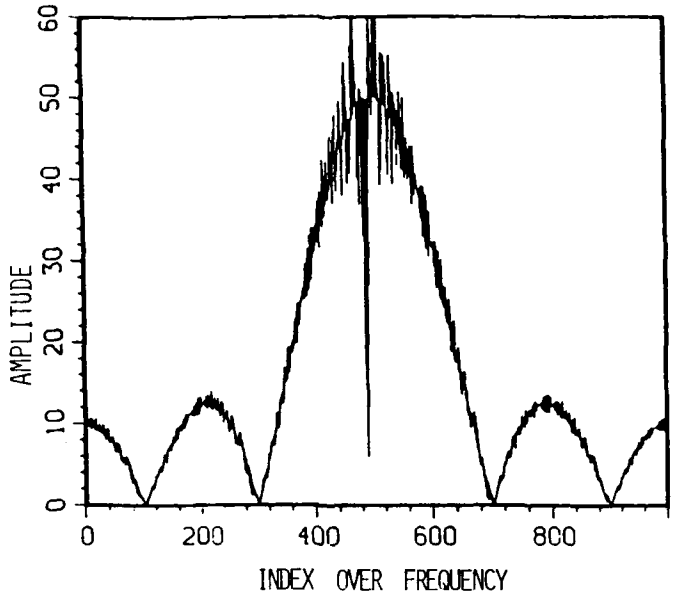

Fig. 2(a) — 100-element Frank code spectrum

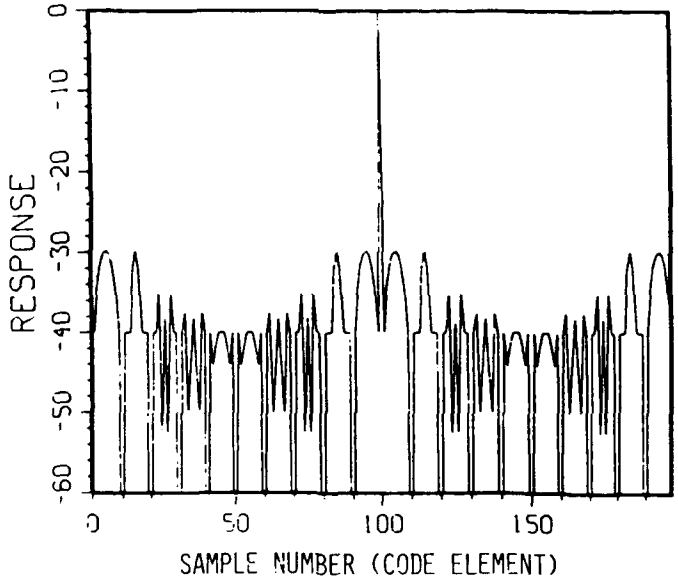

Fig. 2(b) — The matched filter output for the Frank code spectrum of Fig. 2(a)

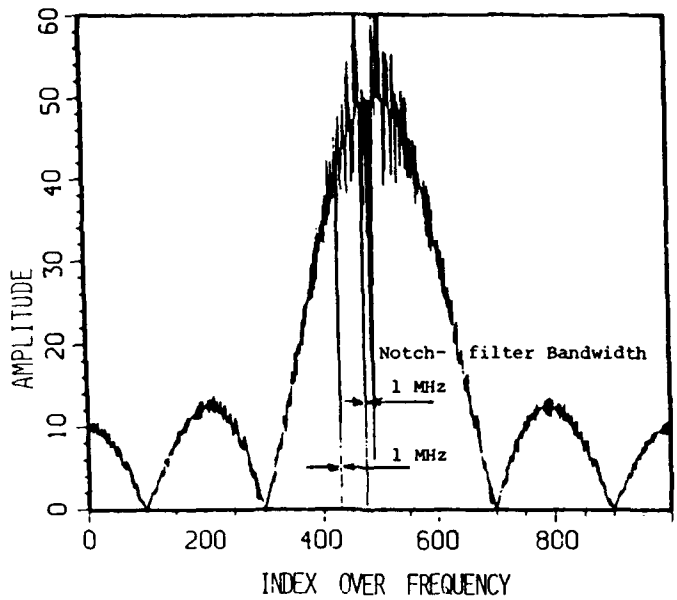

Fig. 3(a) — 100-element Frank code spectrum with very narrow frequency notching

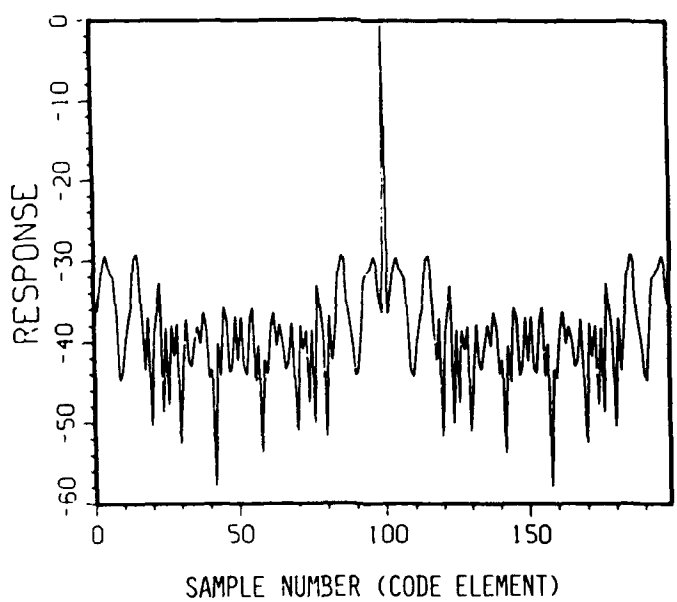

Fig. 3(b) — The matched filter output for the Frank code spectrum of Fig. 3(a)

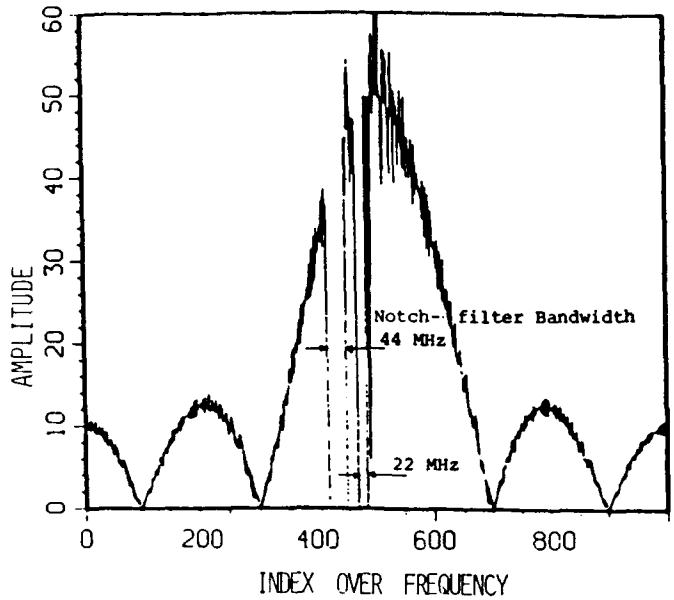

Fig. 4(a) — 100-element Frank code spectrum with very wide frequency notching

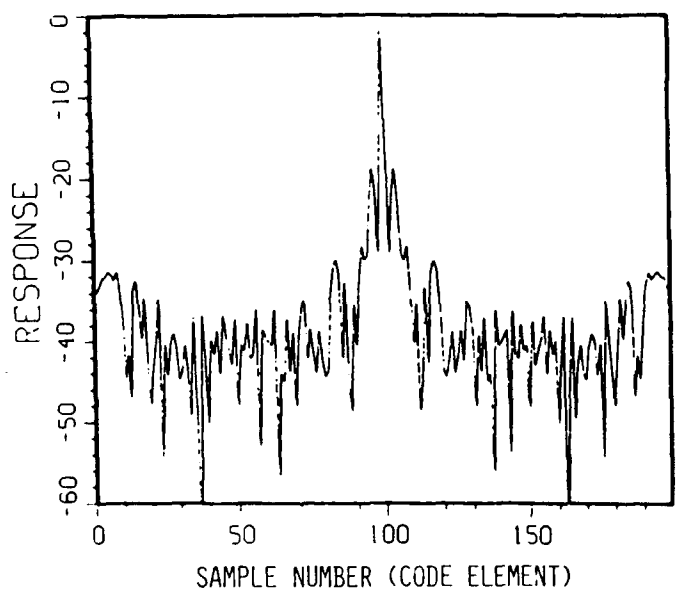

Fig. 4(b) — The matched filter output for the Frank code spectrum of Fig. 4(a)

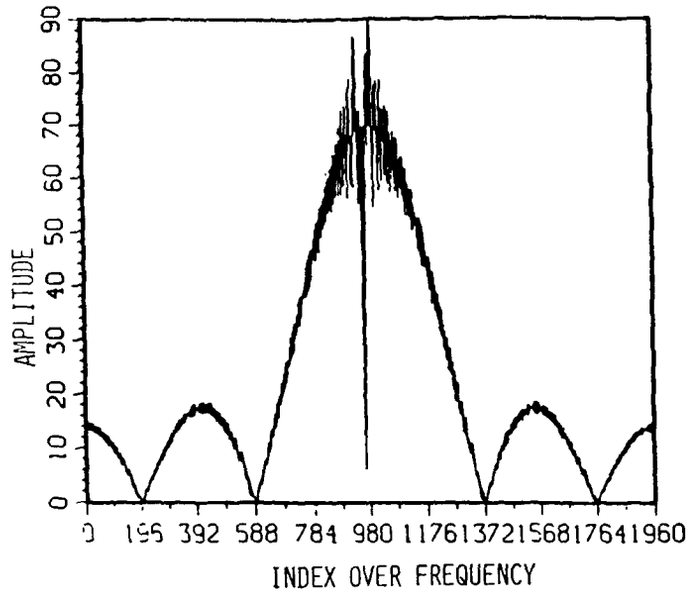

Fig. 5(a) — 196-element Frank code spectrum

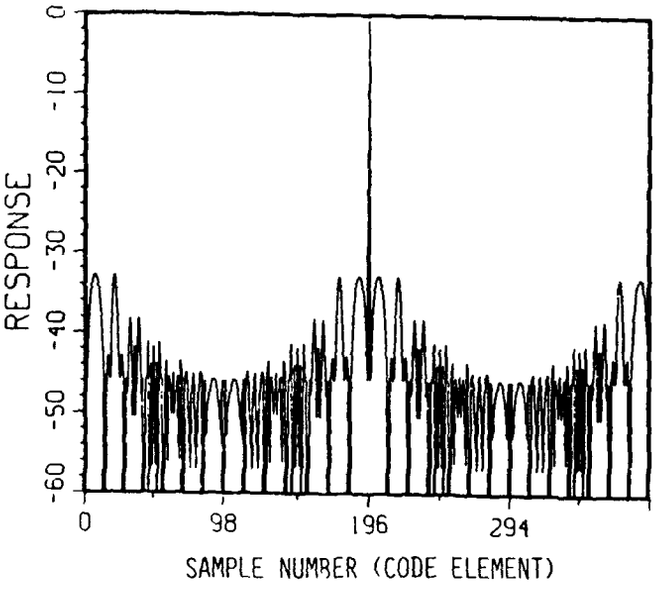

Fig. 5(b) — The matched filter output for the Frank code spectrum of Fig. 5(a)

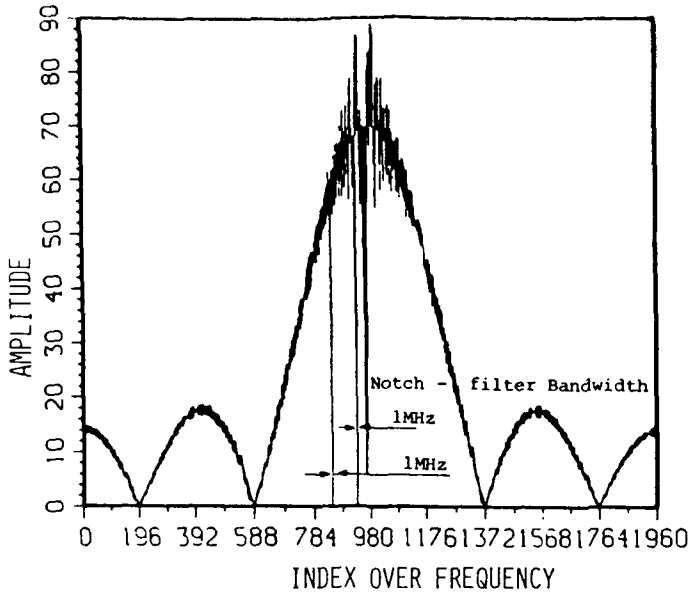

Fig. 6(a) — 196-element Frank code spectrum with very narrow frequency notching

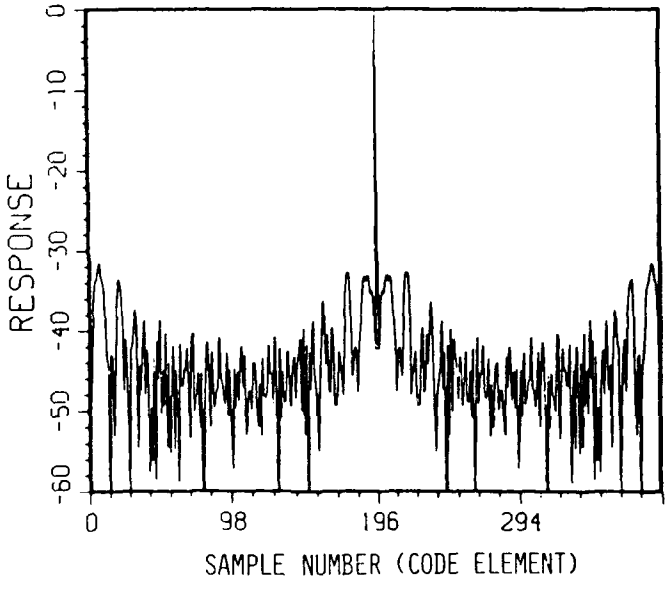

Fig. 6(b) — The matched filter output for the Frank code spectrum of Fig. 6(a)

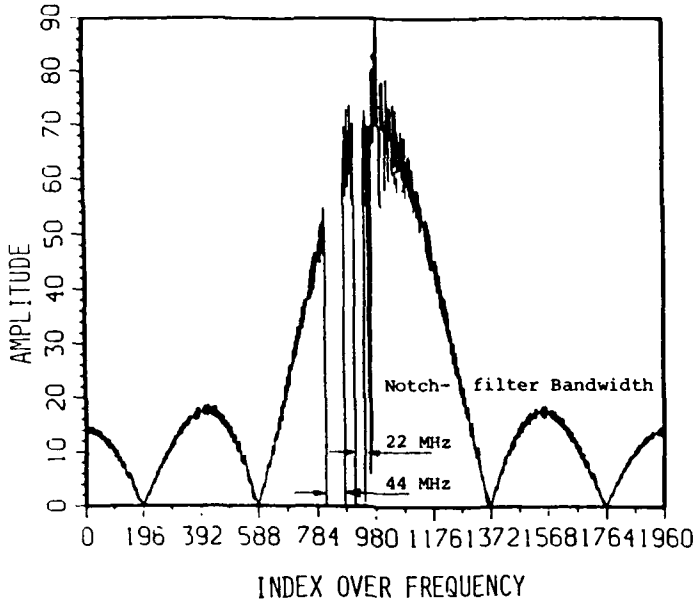

Fig. 7(a) — 196-element Frank code spectrum with very wide frequency notching

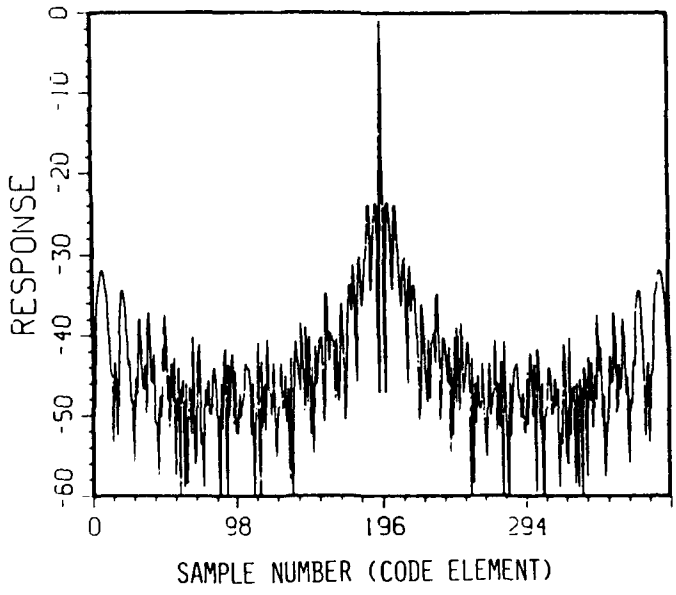

Fig. 7(b) — The matched filter ouput for the Frank code spectrum of Fig. 7(a)

3. A FUNDAMENTAL APPROACH TO ELIMINATING EMI

Pulse compression waveforms are often required in a modern radar design. It may, however, degrade the radar performance if a conventional methodology is used for eliminating EMI such as discussed in Section 2. Among the pulse compression waveforms, the signals derived from orthogonal matrices show potential applications in eliminating the multiple time-around clutter [4, 7]. As to solving EMI problems, we further examine these characteristic waveforms and propose a fundamental approach to eliminating EMI. We search a large class of signals derived from orthogonal matrices in which the property of *mutual orthogonality* is attained. In doing so, different signals derived in a specific set can be practically assigned to different radars on the same or different platforms. A radar alone processes the signals and suppresses the ambiguous range targets or clutter. Among different radars, interference is eliminated at least over the unambiguous range due to mutual orthogonality of the multiple-pulsed waveforms being used.

3.1 A Class of Complementary Codes

A measure of pulse compression waveforms to resolve signals in the spectral and temporal domains is provided by the receiver matched filter output or the signal ambiguity function,

$$\chi(\tau, \omega) = \left| \int x^*(t)\, x(t+\tau)\, e^{-j\omega t} dt \right|^2. \tag{2}$$

For convenience, we define in (2) that $\chi(\tau,\omega) = \left| \psi(\tau,\omega) \right|^2$. In the absence of noise and Doppler shift ($\omega = 0$), the above function $\psi(\tau,0)$ is actually the signal autocorrelation function. It was shown in [8], for two complementary sequences such as the following pairs of Golay sequences of order 16,

$$\begin{aligned} a &= [1\ 0\ 0\ 0\ 1\ 1\ 0\ 1\ 1\ 0\ 0\ 0\ 0\ 0\ 1\ 0] \\ b &= [0\ 1\ 0\ 0\ 0\ 0\ 0\ 1\ 0\ 1\ 0\ 0\ 1\ 1\ 1\ 0] \end{aligned} \tag{3}$$

that the sum of their autocorrelation functions has zero sidelobes.

Generally the complementary codes are defined to be a complementary set of sequences [9], which can also be represented by an array matrix. For example, referring to the Frank codes described in Eq. (1), we can form a multiple-pulsed waveform that consists of i ($i = 10$) pulses with each pulse compressed by the coded sequences $\{\exp(\phi_{ij});\ j = 1,2,\ldots,10\}$ for $i = 1,2,.,10$. Consequently, the array matrix characterizing this multiple-pulsed waveform has the form of $[a_{ij}]$ with $a_{ij} = \exp(\phi_{ij})$ indicating the respective elements at the ith row and jth column. Incidently, the above polyphase waveform (or the array sequences) is complementary coded and, hence, the sum of the autocorrelation functions of the above individual pulses is zero except at the matched point.

For clarity, we consider another example with a binary signal represented by the following complementary code (in an array matrix form).

$$A = \begin{bmatrix} -1 & -1 & -1 & 1 & 1 & -1 & 1 & 1 \\ 1 & 1 & 1 & 1 & 1 & 1 & 1 & 1 \\ -1 & -1 & 1 & 1 & -1 & 1 & -1 & 1 \\ 1 & -1 & -1 & -1 & 1 & 1 & -1 & 1 \\ 1 & 1 & -1 & 1 & -1 & -1 & -1 & 1 \\ -1 & 1 & -1 & -1 & -1 & 1 & 1 & 1 \\ -1 & 1 & 1 & -1 & 1 & -1 & -1 & 1 \\ 1 & -1 & 1 & -1 & -1 & -1 & 1 & 1 \end{bmatrix}.$$

Figure 8 shows the aperiodic autocorrelation function of the above signal. It can be seen, to the maximum unambiguous range interval, that the sum of the autocorrelation functions of all array sequences is zero except at the matched point. Note that the correlation functions appearing in the second, third, . . . time-around intervals are generally nonzeros.

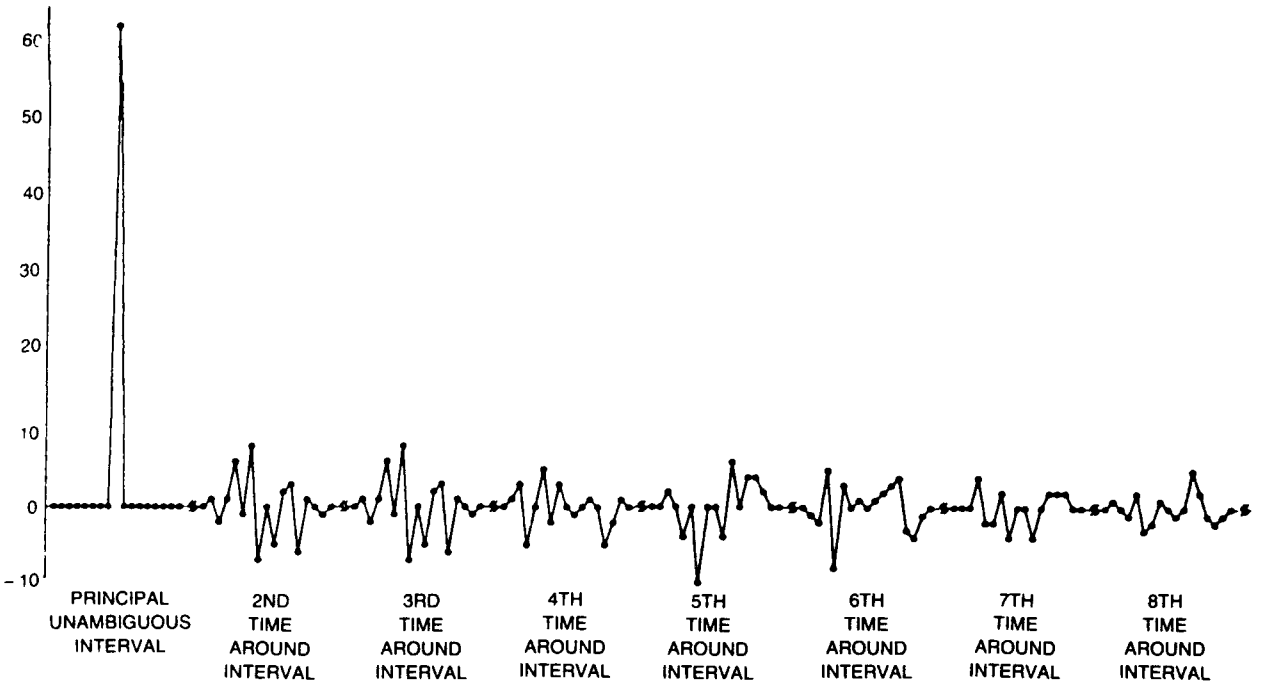

Fig. 8 — A periodic autocorrelation of the multiple signals represented by the complementary array code A

A matrix to be sufficiently a complementary array must be an orthogonal matrix in a sense that the column vectors of the matrix are mutually orthogonal [4]. Consequently, the Hadamard matrices, the Frank and P_4 code square matrices, and matrices generated from a pseudorandom shift register code (such as A above) contain complementary sequences. Matrix A is formed after permutation by a 7×7 submatrix consisting of a simple pseudorandom code ($1 \quad -1 \quad -1 \quad -1 \quad 1 \quad 1 \quad -1$) and its rotations and an eighth row and column of 1s.

It is interesting, as noted in Ref. 4, that the polyphase Frank code and P_4 code square matrices, when considered as multiple-pulsed waveforms, have zero autocorrelation (in a periodic sense) beyond the maximum unambiguous range. Therefore when the signal is continuously transmitted (in a periodic sense) and matched to the reference for a specific range interval, then the stationary clutter from the mismatched range interval is eliminated. If the filter is matched to the most recently transmitted code, the sidelobes of stationary targets in the unambiguous range are zeros. In a sense of zero cross-correlation, instead of zero autocorrelation, the above complementary coded waveforms may be applied to a multisensor operation so that EMI is eliminated. However, a search of "orthogonal sets" containing similar complementary-coded signals is needed. Consequently, different signals in a derived set can be assigned to different radars in which the applied signals are mutually orthogonal. Interference is therefore eliminated among different radar sources.

An orthogonal set S may be formed through orthogonal transformation of a specific array matrix of interest. For example, let the following A_o be a $k \times n$ complementary array matrix (here, $k = n = 4$) and $S = \{A_1, A_2, \ldots\}$ for which $A_1, A_2, \ldots$ are the matrices to be searched for:

$$A_o = \begin{bmatrix} -1 & -1 & 1 & 1 \\ 1 & -1 & -1 & 1 \\ -1 & 1 & -1 & 1 \\ 1 & 1 & 1 & 1 \end{bmatrix}. \tag{4}$$

Then one possible S (corresponding to a Walsh vector set W) can be obtained by $A_i = A_o T_i$ with T_i an $n \times n$ diagonal matrix and $T_i I = V_i \in W$, where V_i is a Walsh vector and I is an n-dimensional identity vector. The procedures, with A_o given above, are illustrated as follows. For a Walsh vector set defined by $W = \{V_1, V_2, V_3, V_4\}$ with $V_1 = (1\ 1\ 1\ 1)^T$, $V_2 = (1\ 1\ -1\ -1)^T$, $V_3 = (1\ -1\ 1\ -1)^T$, and $V_4 = (-1\ 1\ 1\ -1)^T$, we can easily derive that

$$A_1 = \begin{bmatrix} -1 & -1 & 1 & 1 \\ 1 & -1 & -1 & 1 \\ -1 & 1 & -1 & 1 \\ 1 & 1 & 1 & 1 \end{bmatrix}, \tag{5}$$

$$A_2 = \begin{bmatrix} -1 & -1 & -1 & -1 \\ 1 & -1 & 1 & -1 \\ -1 & 1 & 1 & -1 \\ 1 & 1 & -1 & -1 \end{bmatrix}, \tag{6}$$

$$A_3 = \begin{bmatrix} -1 & 1 & 1 & -1 \\ 1 & 1 & -1 & -1 \\ -1 & -1 & -1 & -1 \\ 1 & -1 & 1 & -1 \end{bmatrix}, \tag{7}$$

and

$$A_4 = \begin{bmatrix} 1 & -1 & 1 & -1 \\ -1 & -1 & -1 & -1 \\ 1 & 1 & -1 & -1 \\ -1 & 1 & 1 & -1 \end{bmatrix}. \tag{8}$$

In the above, $S = \{A_1, A_2, A_3, A_4\}$ and the multiple-pulsed waveforms represented by the matrices A_1, A_2, A_3 and A_4 are mutually orthogonal. In other words, any pair of the signals with their representing matrices belonging to S have zero cross-correlation functions. Moreover, each signal is represented by an orthogonal matrix so that its autocorrelation is zero except at the matched point. Figure 9 is the aperiodic autocorrelation function for the signal represented by A_2. Figure 10 illustrates aperiodic cross-correlation between signals represented by A_2 and A_3.

In the example shown above, the derived set S is not unique. For instance, let the Walsh vector be $\tilde{W} = \{V_1, \tilde{V}_2, \tilde{V}_3, V_4\}$, or $\hat{W} = \{V_1, \hat{V}_2, \hat{V}_3, V_4\}$ with $V_1 = [-1\ -1\ -1\ -1]^T$, $\tilde{V}_2 = [-1\ -1\ 1\ 1]^T$, $\tilde{V}_3 = [-1\ -1\ -1\ 1]^T$, and $\hat{V}_4 = [1\ -1\ -1\ 1]^T$. Then two more sets containing mutually orthogonal signals are obtained. In fact, a total of 32 sets can be found in this

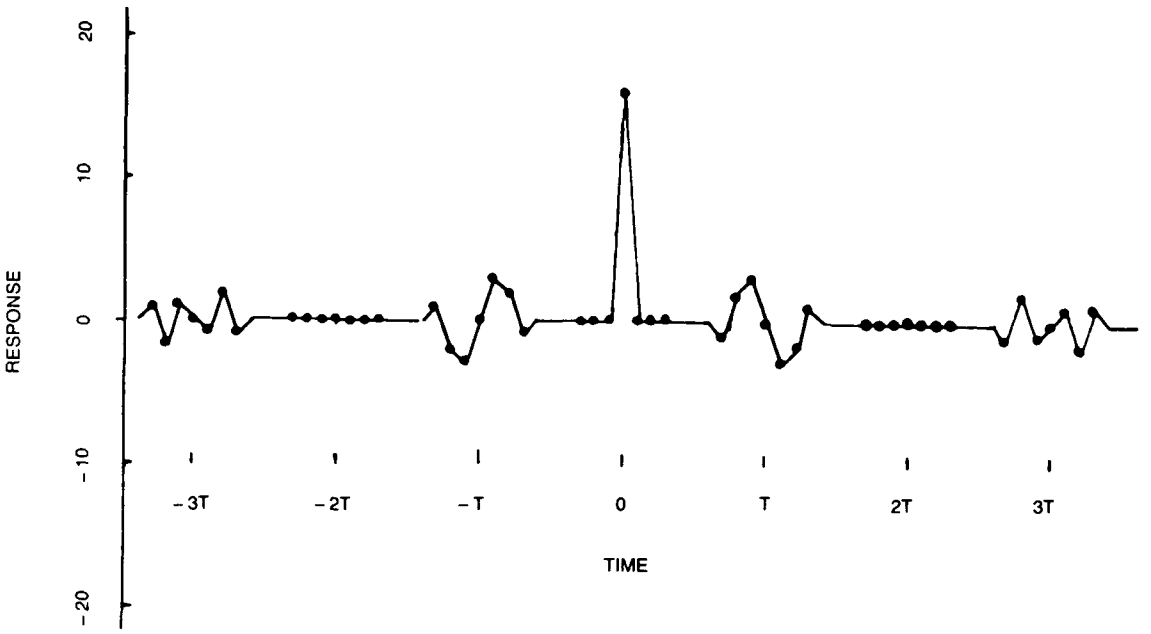

Fig. 9 — A periodic autocorrelation of the multiple signals A_2

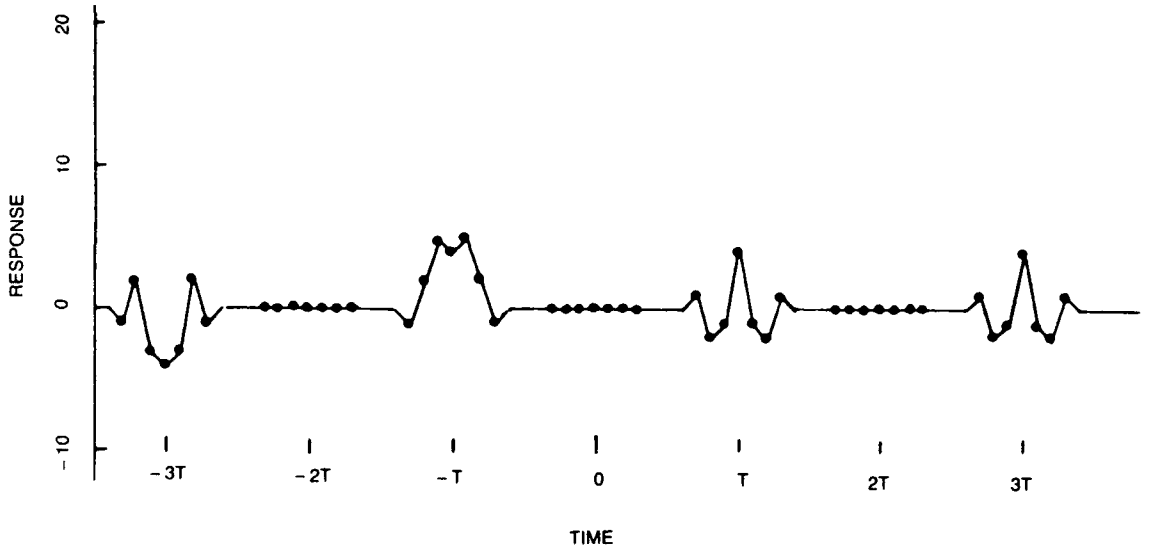

Fig. 10 A periodic cross-correlation between the multiple signals A_2 and A_3

example. The above procedures can be applied to a different seed matrix $\tilde{A}_o$ to obtain a new class of multiple-pulsed signals of interest. If A_o is a polyphase Frank code matrix, additional properties, such as the periodic autocorrelation functions being zero over ambiguous range intervals, are observed.

3.2 Advanced Waveform Synthesis

As discussed in previous sections, mutually orthogonal waveforms are fundamentally applicable in solving EMI problems. With appropriate use of multiple-pulsed signals selected from a derived orthogonal set containing complementary codes, the radar could suppress interference from other radar sources and possibly eliminate ambiguous range targets or clutter. However, orthogonality of the complementary codes are not preserved in the presence of Doppler shift. That is, the temporal sidelobes of matched filter outputs are no longer zeros. The compressed pulse peak is also reduced. For example, if the Doppler shift in angle is π for the separation between two complementary sequences, then the sidelobes of the autocorrelation of these two sequences will add up instead of subtract from each other. To minimize this problem, we examine the option of using orthogonal multiple-pulsed waveforms incorporated with an inner-outer coding scheme. Here a train of pulses, called the outer code, is "modulating" previously discussed complementary codes (the inner code). The inner code sequences are indeed "determined" by a preselected outer code as described next. The outer code may also be called a *macro-sequence* [10].

A synthesized pulse train is simply shown in Fig. 11. The pulse train consists of N_2 pulses with a pulse repetition interval T. Each pulse is pulse-compressed by a complementary sequence confined to a generalized array matrix. The selection of which complementary sequence to be modulated is determined by a predefined outer code. Assume each complementary sequence has N_1 subpulses with a subpulse length of δ (see Fig. 11). Then, for the kth pulse,

$$u_k = \sum_{n=0}^{N_1-1} h_n(t) e^{j\theta_n},$$

where $h_n(t) = 1$ and $\theta_n = 0$ or π with $n\delta \le t < (n+1)\delta$ and $n = 0, 1, \ldots, N_1 - 1$. We denote the resulting waveform by $\sum_{k=0}^{N_2-1} u_k(t)$ with $kT \le t < kT + N_1\delta$ and $k = 0, 1, \ldots, N_2 - 1$.

According to Eq. (2), the matched filter outputs are related to

$$\psi(\tau, \omega) = \int_0^{N_2 T} \sum_{k=0}^{N_2-1} u_k^*(t)\, u_k(t + \tau) e^{j\omega t} dt \tag{9}$$

or

$$\psi(\tau, \omega) = \sum_{k=0}^{N_2-1} \int_{kT}^{KT+N_1\delta} u_k^*(t - kT)\, u_k(t - kT + \tau) e^{j\omega t} dt. \tag{10}$$

By replacing the parameter $t - kT$ by $\hat{t}$, the above equation becomes

$$\psi(\tau, \omega) = \sum_{k=0}^{N_2-1} \int_0^{N_1\delta} u_k^*(\hat{t})\, u_k(\hat{t} + \tau) e^{j\omega\hat{t}} e^{j\omega kT} d\hat{t}$$

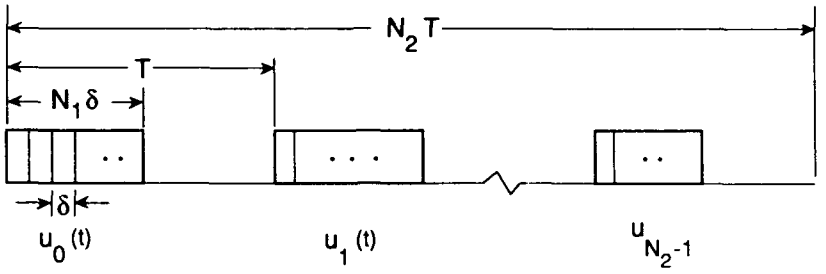

Fig. 11 — A synthesized pulse train

or

$$\psi(\tau, \omega) = \sum_{k=0}^{N_2-1} U_k e^{j\omega kT} \tag{11}$$

where

$$U_k = \int_0^{N_1\delta} u_k^*(\hat{t})\, u_k(\hat{t} + \tau) e^{j\omega\hat{t}} d\hat{t}. \tag{12}$$

The results of Eqs. (11) and (12) are particularly interesting since their explicit forms can be easily analyzed. As noted above, the assignment of u_k is determined by a predefined outer code m_k. To be general, we consider the complementary array matrix has the order of $4 \times N_1$ and is represented by an array matrix $(a(t)\ b(t)\ c(t)\ d(t))^T$. Consequently, one of the four complementary sequences would be assigned to u_k where $k = 1,2, \ldots, N_2$. Naturally, a good choice of the outer code m_k is the Quadraphase sequence that can be generated by the Barker code or any other binary-phase codes [11] if a longer code length is desirable. Here u_k is assigned as follows: $u_k = a(t)$, $b(t)$, $c(t)$ or $d(t)$ if $m_k = 1, -1, j$ or $-j$, respectively.

As a result, Eq. (12) can be rewritten as

$$\begin{aligned} U_k = \int_0^{N_1\delta} & \left[\frac{(m_k^2 + 1)(m_k + 1)}{4} a^*(t) + \frac{(m_k^2 + 1)(m_k - 1)}{-4} b^*(t) \right. \\ & \left. + \frac{(m_k^2 - 1)(m_k + j)}{-4j} c^*(t) + \frac{(m_k^2 - 1)(m_k - j)}{4j} d^*(t) \right] \\ & \times \left[\frac{(m_k^2+1)(m_k+1)}{4} a(t+\tau) + \frac{(m_k^2 + 1)(m_k - 1)}{-4} b(t + \tau) \right. \\ & \left. + \frac{(m_k^2 - 1)(m_k + j)}{-4j} c(t + \tau) + \frac{(m_k^2 - 1)(m_k - j)}{4j} d(t + \tau) \right] e^{j\omega t} dt \ . \end{aligned} \tag{13}$$

If we consider the matched filter outputs in the unambiguous range interval only, then

$$\psi(\tau,\omega) = \sum_{k=0}^{N_2-1} \left[\frac{(m_k^2+1)^2(m_k+1)^2}{16}\psi_a(\tau,\omega) + \frac{(m_k^2+1)^2(m_k-1)^2}{16}\psi_b(\tau,\omega) + \frac{(m_k^2-1)^2(m_k+j)^2}{-16}\psi_c(\tau,\omega) + \frac{(m_k^2+1)^2(m_k-j)^2}{-16}\psi_d(\tau,\omega)\right] e^{j\omega Tk}, \quad (14)$$

where $\psi_a(\tau,\omega) = \int a^*(t)\, a(t+\tau)e^{j\omega t}dt$. The same definitions apply to $\psi_b(\tau,\omega)$, $\psi_c(\tau,\omega)$ and $\psi_d(\tau,\omega)$.

After simplification, one can easily derive

$$\begin{aligned}\psi(\tau,\omega) = {} & \frac{1}{4}(\psi_a(\tau,\omega)+\psi_b(\tau,\omega)+\psi_c(\tau,\omega)+\psi_d(\tau,\omega))\sum_{k=0}^{N_2-1} e^{j\omega kT} \\ & + \frac{1}{4}(\psi_a(\tau,\omega)+\psi_b(\tau,\omega)-\psi_c(\tau,\omega)-\psi_d(\tau,\omega))\sum_{k=0}^{N_2-1} m_k^2\, e^{j\omega kT} \\ & + \frac{1}{4}(\psi_a(\tau,\omega)-\psi_b(\tau,\omega))\sum_{k=0}^{N_2-1} m_k\, e^{j\omega kT} - \frac{1}{4}(\psi_c(\tau,\omega)-\psi_d(\tau,\omega))\sum_{k=0}^{N_2-1} jm_k e^{j\omega kT} \\ & + \frac{1}{4}(\psi_a(\tau,\omega)-\psi_b(\tau,\omega))\sum_{k=0}^{N_2-1} m_k^3 e^{j\omega kT} + \frac{1}{4}(\psi_c(\tau,\omega)-\psi_d(\tau,\omega))\sum_{k=0}^{N_2-1} jm_k^3 e^{j\omega kT} \end{aligned} \quad (15)$$

and

$$\begin{aligned}|\psi(\tau,\omega)| \le {} & \frac{1}{4}\left|(\psi_a(\tau,\omega)+\psi_b(\tau,\omega)+\psi_c(\tau,\omega)+\psi_d(\tau,\omega))\right| \left|\sum_{k=0}^{N_2-1} e^{j\omega kT}\right| \\ & + \frac{1}{4}\left|(\psi_a(\tau,\omega)+\psi_b(\tau,\omega)-\psi_c(\tau,\omega)-\psi_d(\tau,\omega))\right| \left|\sum_{k=0}^{N_2-1} m_k^2 e^{j\omega kT}\right| \\ & + \frac{1}{4}\left|(\psi_a(\tau,\omega)-\psi_b(\tau,\omega)-\psi_c(\tau,\omega)+\psi_d(\tau,\omega))\right| \left|\sum_{k=0}^{N_2-1} m_k e^{j\omega kT}\right| \\ & + \frac{1}{4}\left|(\psi_a(\tau,\omega)-\psi_b(\tau,\omega)+\psi_c(\tau,\omega)-\psi_d(\tau,\omega))\right| \left|\sum_{k=0}^{N_2-1} m_k^3 e^{j\omega kT}\right|. \end{aligned} \quad (16)$$

In Eq. (16), the summation terms are in DFT format, and hence $\psi(\tau,\omega)$ can be easily calculated if the complementary array matrices and outer codes $\{m_k\}$ are given.

In Eq. (16), one can also show that

$$\left| \sum_{k=0}^{N_2-1} e^{j\omega kT} \right| = \frac{\sin N_2 \pi z}{\sin \pi z} \tag{17}$$

where $\omega = 2\pi f$, and $z = fT$ is a normalized frequency parameter. If the Quadraphase sequence $\{m_k\}$ is generated from a 13-element Barker code (that is, $\{m_k\} = \{1, j, -1, -j, 1, -j, 1, -j, 1, -j, -1, j, 1\}$), then as derived in Ref. 11,

$$\left| \sum_{k=0}^{N_2-1} m_k e^{j\omega kT} \right| = \left(12 + \frac{\cos 26\pi z}{\cos 2\pi z} \right)^{1/2}. \tag{18}$$

We can also easily derive that

$$\left| \sum_{k=0}^{N_2-1} m_k^2 e^{j\omega kT} \right| = \begin{cases} \dfrac{\cos N_2 \pi z}{\cos \pi z}, & N_2 = odd \\ \dfrac{\sin N_2 \pi z}{\cos \pi z}, & N_2 = even \end{cases} \tag{19}$$

and

$$\left| \sum_{k=0}^{N_2-1} m_k^3 e^{j\omega kT} \right| = \left| \sum_{k=0}^{N_2-1} m_k e^{j\omega kT} \right| = \left((N_2 - 1) + \frac{\cos 2N_2 \pi z}{\cos 2\pi z} \right)^{1/2}. \tag{20}$$

For this specific case, with the analytical results shown in Eqs. (15) through (20), the matched filter response can easily be realized.

To further evaluate these synthesized waveforms and compare the results consistently, we determine the matched filter outputs at the presence of Doppler shift for the following cases that the outer codes are: (a) simply two pulses, (b) a special case of the Quadraphase sequence generated from a 13-element Barker code, (c) the derived sequence of case (b) plus $-j$, and (d) a complementary sequence (generated by a pseudorandom sequence plus one). In all cases, we select the complementary array matrix A_o to be the Golay mates of order 16, that is $A_o = (a\ b)^T$ with a and b defined in Eq. (3). These two complementary sequences (the inner code) are then modulated by the outer code, which has a pulse repetition period of T and a duty cycle of 50%. A computer program closely following Eq. (11) is used to generate the matched filter outputs for the above cases. The Doppler phase shifts ϕ are referenced to the entire code length N_2T, i.e., $\phi = 2\pi f(N_2T)$ and is varied from 0 to approximately π.

Case A : This is the baseline case where the pulse train contains $a(t)$ and $b(t)$ only. In this case, the matched filter outputs are very much affected by the Doppler shift. According to Eq. (11),

$$\psi(\tau, z) = U_0(\tau, z) + U_1(\tau, z)\, e^{j2\pi z}. \tag{21}$$

Clearly, $\psi(\tau,z) = U_0(\tau,z) + U_1(\tau,z)$ or $\psi(\tau,z) = U_0(\tau,z) - U_1(\tau,z)$ when $z = 0$ or $1/2$. Figure 12 shows the 3-D matched-filter output response $|\psi(\tau,z)|^2$. In the figures, there are 31 (or $2 \times 16 - 1$) samples in the time axis and 51 samples in the frequency axis. The magnitude is normalized to the response peak at $\tau = z = 0$, i.e., $\chi_{max} = N_1^2 N_2^2$.

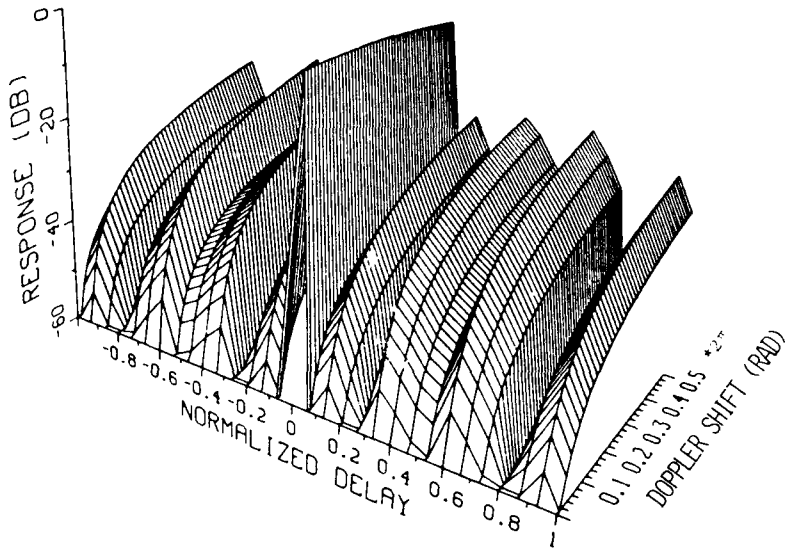

Fig. 12 — Ambiguity diagram of the Golay complementary sequences of length 16

Case B : Here we consider the outer code to be a special case of the Quadraphase sequence generated from a 13-element Barker code. We assume the assigned complementary sequences are $a(t)$, $b(t)$, $a(t)$, and $b(t)$ when the outer code $m_k = 1, -1, j$ and $-j$, respectively. This results in $\psi_a(\tau, z) = \psi_c(\tau, z)$ and $\psi_b(\tau, z) = \psi_d(\tau, z)$ in Eq. (14), and Eq. (15) becomes

$$\left|\psi(\tau, z)\right| \leq \frac{1}{2}(\psi_a + \psi_b)\left|\sum_{k=0}^{N_2-1} e^{j\omega kT}\right| + \frac{1}{2}(\psi_a - \psi_b)\left|\sum_{k=0}^{N_2-1} m_k^3 e^{j\omega kT}\right| . \tag{22}$$

With Eqs. (19) and (20), Eq. (22) can be further simplified to

$$\left|\psi(\tau, z)\right| \leq \frac{1}{2}(\psi_a + \psi_b)\frac{\sin 13\pi z}{\sin \pi z} + \frac{1}{2}(\psi_a - \psi_b)\left(12 + \frac{\cos 26\pi z}{\cos \pi z}\right)^{1/2} . \tag{23}$$

It is interesting to see that the matched filter outputs are composed of the sum and difference of the autocorrelation functions of complementary sequences weighted by $w_1 = \sin 13\pi z/\sin \pi z$ and $w_2 = (12+\cos 26\pi z/\cos \pi z)^{1/2}$, respectively.

When $\tau \neq 0$, $\psi_a + \psi_b$ is small due to the property of complementary sequences. The filter output result hence depends on the second term in which some sidelobes of $\psi_a - \psi_b$ are usually not identically zeros. Clearly the second term, and hence the matched filter output, is minimized if we can find a good outer code such that the weight of $\psi_a - \psi_b$ is relatively *flat and bounded.* It is indeed the case here. Figure 13 shows the ambiguity diagram of the Golay sequences of length 16 outercoded by a modified Quadraphase code. It appears that the output responses, except at zero Doppler shift, demonstrate much better performance compared with that shown in Case A. For example, for a Doppler shift of 0.8π over the entire pulse train, the main peak sidelobe is about -47 dB compared to -19 dB in Fig. 12 of Case A. In both cases, the reduction of the matched main peak is nearly the same.

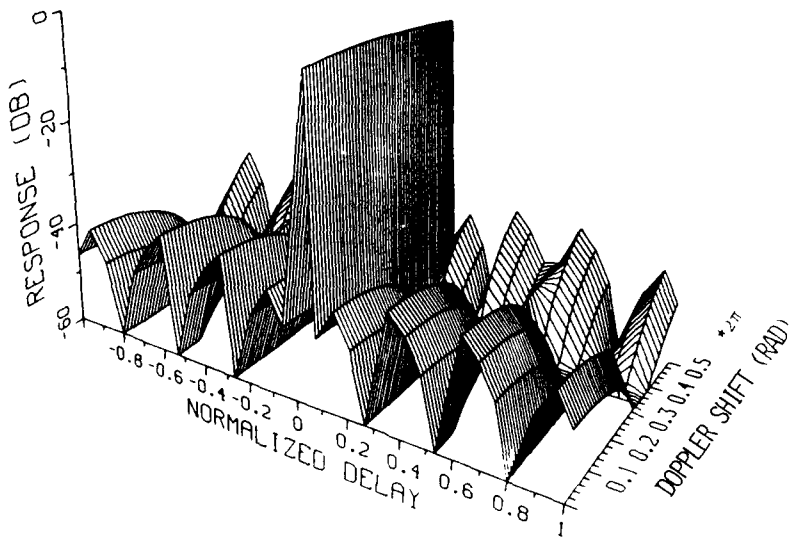

Fig. 13 — Ambiguity diagram of the Golay sequences outercoded by a modified Quadraphase code

Note that the weighting function w_1 is oscillatory having nulls at the frequencies of $z = n/13$, $n = 1, 2, \ldots$ Even at the matched point $\tau = 0$, the result of $\tau = 0$ is expected at the above frequencies. Also, in the above, the resulting synthesized waveform is actually a binary sequence (due to simplification) and $\{m_k\} = \{a, a, b, b, a, b, a, b, a, b, b, a, a\}$. There are 7 a's and 6 b's in the sequence. The unequal numbers of a and b result in *nonzero* sidelobes of the matched filter output at zero Doppler shift (Fig. 13).

Case C : In this case, we form a new outer code, i.e., $1, j, -1, -j, 1, -j, 1, -j, 1, -j, -1, j, 1, -j$, which is obtained by adding $-j$ to the previous Quadraphase sequence generated from a 13-element Barker code. In other words, one more pulse coded by b is concatenated to the binary sequence $\{m_k\}$ derived in Case B. The resulting sequence contains equal numbers of a's and b's. Zero sidelobe response is thus preserved for the matched filter output when the Doppler shift is absent. Figure 14 shows the ambiguity diagram of this synthesized waveform. Clearly the matched filter outputs for this synthesized waveform perform superior to the corresponding ones as seen in Cases A and B.

Case D : The case that the outer code be a complementary as suggested in Ref. 11 is simulated here. We select the outer code S as a pseudorandom sequence plus one. For the code length to be closer to 14 as used in the previous examples, we consider that the pseudorandom sequence has a code length of 15 and is generated by a polynomial of 023 in octal. We also choose the initial condition of 7 in octal, which results in a lowest peak sidelobe of 3 or of 10 log $(3/15)^2$ dB as normalized to the mainlobe peak. It is easy to derive that $S = \{0\ 1\ 1\ 1\ 1\ 0\ 1\ 0\ 1\ 1\ 0\ 0\ 1\ 0\ 0\ 0\}$. With this outer code modulating the complementary sequences a and b, the matched filter output response is shown in Fig. 15. As before, we vary the Doppler shift over the entire pulse train from 0 to π. The results show improvement in radar performance but are not as good as in Case C when both are compared to the baseline Case A.

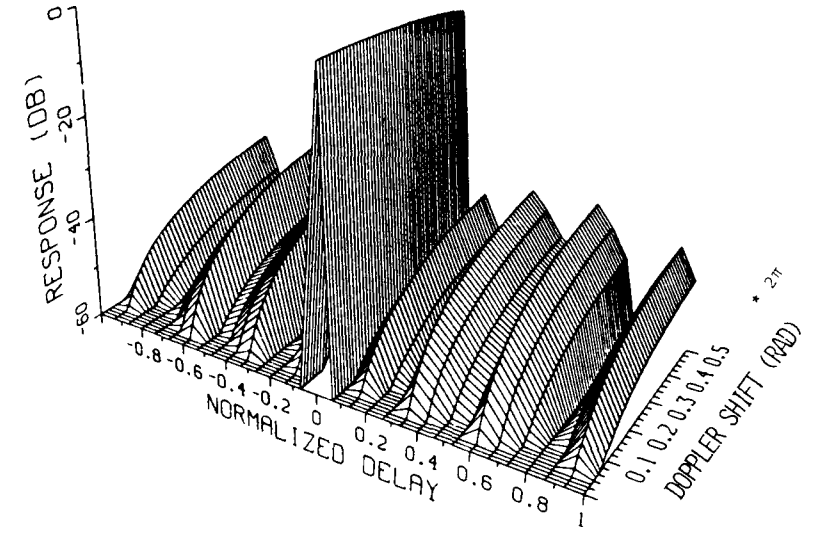

Fig. 14 — Ambiguity diagram of the Golay sequences outercoded by a modified Quadraphase code

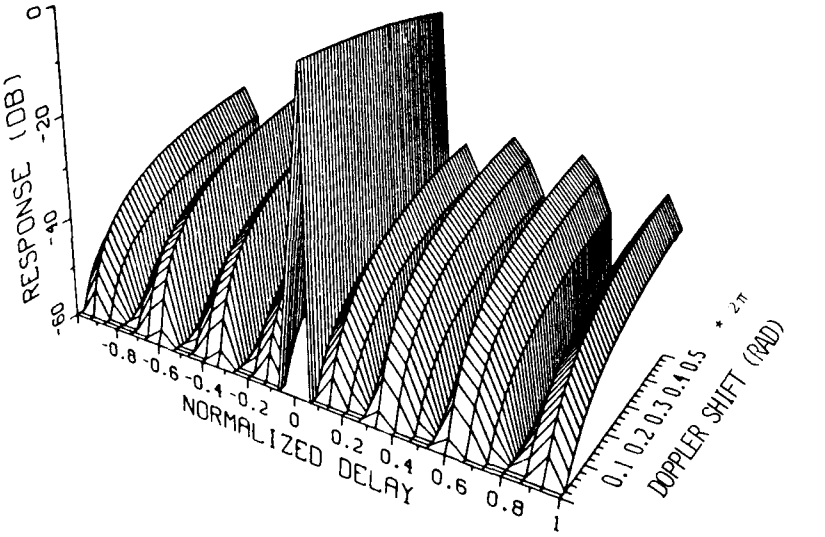

Fig. 15 — Ambiguity diagram of the Golay sequences outercoded by a 16-element complementary sequence

4. DISCUSSION AND CONCLUSIONS

In this report, use of radar pulse compression against EMI is analyzed. We show that mutually orthogonal waveforms specifically derived from complementary coded signals are fundamentally applicable in solving EMI problems without degrading the radar performance. We consider transmitted multiple-pulsed (dissimilar) waveforms as a burst of pulses that are pulse-compressed by complementary sequences. We then search a class of these characterized signals in which the property of *mutual orthogonality* is attained. As a result, different signals in a specifically derived set can be assigned to different radars on the same or different platforms in which the signals are mutually orthogonal *in the sense that cross-correlation of signals is zero.* A radar alone processes the signals and suppresses the ambiguous range targets or clutter. Among different radars, interference is eliminated at least over the unambiguous range due to mutual orthogonality of the multiple-pulsed waveforms being used. Synchronization among multiple radars may be effective in reducing problems associated with cross-correlation in different unambiguous range intervals.

However, imperfection of orthogonality is observed in the presence of Doppler shift. In considering severe Doppler shift, Doppler filter bank receivers can be practically implemented to process the target signals. Otherwise, this undesirable effect may be partially compensated for through advanced waveform synthesis. We describe the option of using complementary coded signals incorporated with an inner-outer coding scheme. We generate the characteristic ambiguity diagram of a synthesized waveform composed of a simple pair of Golay sequences outercoded by a pseudorandom-code-generated complementary sequence. If the outer code is chosen from a modified Quadraphase code, even better waveform characteristics can be achieved. Both synthesized waveforms perform superior to the baseline case where the signal is simply two pulses and coded by the Golay sequences.

In conclusion, with appropriate use of the multiple-pulsed waveforms selected from a derived set of complementary coded signals, the radar would suppress interference from other radar sources. In addition, stationary targets or clutter from ambiguous/mismatched range intervals may also be eliminated. In the future, we plan to generalize this fundamental principle, perhaps through waveform synthesis and also to search for best seed matrices and various orthogonal transformations in obtaining new signal sets of interest. It would be ideal if the described zero autocorrelation (except at the matched point) and zero cross-correlation between signals could be extended over ambiguous range intervals and also be valid in the presence of Doppler shift.

5. ACKNOWLEDGMENTS

The author thanks C. L. Temes, L. Cohen, and R. Ford for their helpful discussions on the subject.

6. REFERENCES

1. R.M. Bauman, C.L. Golliday, R.K. Royce, D.C. Andrews, and C.E. Hobbis, "Adaptive Cancellation of Local Electromagnetic Interference in Naval HF Communication Systems," NRL Report 8175, July 1978.

2. D.K. Barton, ed., *Radars Vol 3, Pulse Compression* (Artech House, Inc., Dedham, MA, 1978).

3. B.L. Lewis, F.K. Kretschmer, Jr., and W.W. Shelton, in *Aspects of Radar Signal Processing* (Artech House, Inc., Dedham, MA, 1986).

4. F.K. Kretschmer, Jr. and K. Gerlach, "Radar Waveform Derived from Orthogonal Matrices," NRL Report 9080, Feb. 1989.

5. C.T. Lin, F.C. Lin, and W.L. Thrift, "AN/SPS-49 Waveforms and System Architecture Study," NRL Report 9233, Dec. 1989.

6. Electromagnetic Compatibility Analysis Center, IIT Research Institute Report ECAC-CR-87-008, "EMC Analysis of the AN/SPS-49(V)-X Radar with Civilian Air Traffic Control Receivers," 1987.

7. G. Weathers and E.M. Holiday, "Group-Complementary Array Coding for Radar Clutter Rejection," *IEEE Trans. on AES*, May 1983.

8. M.J.E. Golay, "Complementary Series," *IRE Trans. Inf. Theory* **IT-7**, 1961.

9. C.C. Tseng and C.L. Liu, "Complementary Set of Sequence," *IEEE Trans. Inf. Theory* **IT-18**(5), 1972.

10. S.Z. Budisin, B.M Popovic, I.M. Indjin, "Design Radar Signals Using Complementary Sequences," International Radar Conference, 1987.

11. J.W. Taylor, Jr. and H.J. Blinchikoff, "Quadraphase—A Radar Pulse Compression Signal with Unique Characteristics," *IEEE Trans. on AES*, March 1988.